A combined experimental-numerical investigation of two-phase self-cleaning drop modulation by amphiphilic component addition

frontiers | Frontiers in Chemical Engineering

TYPE Brief Research Report
PUBLISHED 12 December 2025
DOI 10.3389/fceng.2025.1640523

OPEN ACCESS

EDITED BY
Yusha Hu,
Hong Kong Polytechnic University, Hong Kong SAR, China

REVIEWED BY
Vickramjeet Singh,
Dr. B. R. Ambedkar National Institute of Technology Jalandhar, India
Iman El Mahallawi,
Cairo University, Egypt

*CORRESPONDENCE
Henrik Ström,
henrik.strom@chalmers.se

RECEIVED 03 June 2025
REVISED 28 November 2025
ACCEPTED 03 December 2025
PUBLISHED 12 December 2025

CITATION
Kumar SV and Ström H (2025) A combined experimental-numerical investigation of two-phase self-cleaning drop modulation by amphiphilic component addition.
Front. Chem. Eng. 7:1640523.
doi: 10.3389/fceng.2025.1640523

A combined experimental-numerical investigation of two-phase self-cleaning drop modulation by amphiphilic component addition

Shreyas Vijayendra Kumar and Henrik Ström*

Division of Fluid Dynamics, Department of Mechanics and Maritime Sciences, Chalmers University of Technology, Gotheburg, Sweden

Industrial plate heat exchangers for cooling of complex, condensing gas mixtures are possible to operate in a self-cleaning mode if a stable flow of small, spherical-like, motile drops can be realized over the heat transfer surfaces. Here, we investigate the effects of adding an amphiphilic component (benzoic acid) to a pure air/water system in terms of providing the necessary prerequisites for such a functionality. The equilibrium apparent (static) advancing and receding contact angles are measured experimentally at varying inclinations and used to inform multiphase direct numerical simulations using the Volume-of-Fluid method. The simulations enable quantification of the distortion of drops caused by the combined gas-liquid-plate interaction in the presence of flow. It is found that the addition of benzoic acid lowers the apparent contact angles, and that the magnitude of this effect is dependent on the plate surface treatment – being more pronounced on a hydrophobically modified plate than on a hydrophilically modified one. The addition of benzoic acid increases the wetting of the drop on the surface and decreases the flow-exposed gas-liquid interface, although both these effects are relatively modest in magnitude. It is suggested that two-phase heat exchangers relying on self-cleaning mechanisms are relatively immune to the presence of low concentrations of amphiphilic impurities that are chemically similar to benzoic acid. The present work thus highlights the role of combined experimental-numerical approaches to gain insight into process phenomena that are not readily amenable to only experiments or only modeling.

KEYWORDS

benzoic acid, computational fluid dynamics, contact angle, hydrophobic, two-phase flow

1 Introduction

Cooling of hydrocarbon-rich gas mixtures is common in many industrial processes, for example, in upgrading and heat recovery of product gases from thermochemical conversion of biomass (Thunman et al., 2018). Such cooling processes are associated with severe challenges related to fouling and deterioration of process equipment, as heavier compounds involving aromatic rings (collectively known as tars) may stick to heat transfer surfaces as they condense (Maggiolo et al., 2019a; Müller-Steinhagen et al., 2011). Such fouling implies a need for constant expensive maintenance of filters, pipes, and overall equipment (Melo et al., 1988) and impedes heat recovery. The need to adapt entire process schemes to avoid

problems with fouling and the suboptimal heat recovery leads to higher investment and running costs (Li et al., 2017; Jordan and Akay, 2013). Researchers and engineers have therefore sought new solutions to heat recovery during hydrocarbon-rich gas cooling, where fouling can be either minimized or mitigated altogether. One such approach is to draw inspiration from surface-modification-based anti-fouling techniques developed for the dairy industry (Santos et al., 2004) or membrane processes (Kochkodan et al., 2014). As tars are typically repelled by water, the formation of a water film (on hydrophilic surfaces) or a droplet-laden "lotus effect"-type of flow (Zhang et al., 2016) (on hydrophobic surfaces) can be hoped to protect the heat transfer surface from tar deposits (Maggiolo et al., 2019a).

Recently, it has been shown that a self-cleaning effect may indeed be realized in plate heat exchangers operated at conditions favorable to promoting the formation of small, spherical-like, motile drops (Maggiolo et al., 2019a; Maggiolo et al., 2019b; Zhang et al., 2019; Hassan et al., 2020; Al-Sharafi et al., 2017) as steam and tars condense (Maggiolo et al., 2019a; Maggiolo et al., 2019b). More specifically, experiments revealed that fouling is significantly reduced on hydrophobically treated plates (whereas severe fouling is observed on untreated ones) after hours of exposure to producer gas from biomass gasification (Maggiolo et al., 2019a). Observation of the plates after the experiments indicated that the condensed droplets are smaller and that the overall hold-up of condensed vapor is lower in the hydrophobically treated plates, indicating a pronounced mobility of droplets. Numerical simulations of the two-phase flow and condensation in the heat exchanger confirmed the effect of wetting on droplet pattern formation, elucidating how vapor condenses in the form of numerous small droplets to collect and remove tars to prevent severe fouling (Maggiolo et al., 2019a).

However, in Maggiolo et al. (2019a), these conclusions were reached through numerical simulations based on physicochemical data for pure air/water systems, and the possible role played by tar components in modulating the contact angles at the three-phase contact line have hitherto been overlooked. Therefore, it is the aim of the present work to investigate the possible modulation of wetting properties imparted by addition of tar-like components to a pure air/water system.

In typical thermochemical conversion processes, the dominant tar species would be benzene and toluene (Thunman et al., 2018). Benzene is carcinogenic (Loomis et al., 2017) and toluene is toxic (Cohr and Stokholm, 1979). In the current work, benzoic acid was therefore chosen as a safer, structurally related compound to benzene and toluene, allowing insight into how aromaticity and limited water solubility affect droplet behavior, while avoiding the toxicity and volatility of the more hazardous industrial analogs. Benzoic acid (C_6H_5COOH) has a benzene ring with a carboxyl substituent, as opposed to pure benzene (C_6H_6; a pure benzene ring) or toluene (C_7H_8; a benzene ring with a methyl substituent). Benzoic acid exhibits amphiphilic behavior: the hydrophobic aromatic ring in benzoic acid preferentially orients towards the gas phase at a gas-liquid interface, while the polar carboxyl group remains in the water (Lu et al., 2024). In terms of hydrophobicity and π-π interactions at the air-water interface, benzoic acid is therefore considered a reasonable proxy for benzene and toluene. However, it should be stressed that the behavior in terms of volatility and vapor-liquid dynamics (which are not the focus of the present work) are not expected to be well representative of water/benzene or water/toluene mixtures. We specifically note that benzoic acid can act as a weak surfactant due to partial ionization, which means that it might lower surface tension in a way that benzene and toluene do not (Phan, 2018). Therefore, the current analysis is designed to be conservative. The elucidation of the role played by benzoic acid at the gas-liquid interface in air-water-plate systems relevant to industrial hydrocarbon-rich gas cooling can therefore provide important first insights into the possible modulation of the self-cleaning effect by surface-active components including aromatic rings at low concentration.

It is known that uncoated steels exposed to benzoic acid solutions tend to attain increased contact angles due to surface adsorption where the carboxyl anchors to the steel and exposes the aromatic ring (Satyarthy et al., 2025; Alamry et al., 2023). Coatings can, however, significantly alter the possibility of surface adsorption and thereby affect the role of benzoic acid in wettability modulation on steel (Kolman and Abbas, 2019). More specifically, addition of benzoic acid increases the contact angle if surface adsorption takes place, whereas it decreases the contact angle if there is no strong interaction with the solid surface as the gas-liquid surface tension is lowered (Kim et al., 2021; Liang and Clarens, 2018).

Here, we perform experimental characterization of the equilibrium contact angles for drops placed on steel plates, treated to be either more hydrophilic or more hydrophobic than conventional steel. We systematically quantify the effect of adding benzoic acid to distilled water on the equilibrium contact angles of drops placed on either of the two plates.

Thereafter, we perform multiphase direct numerical simulations of drop motion in a doubly periodic channel that mimics a straight section of a plate heat exchanger. We enforce the experimentally derived contact angles and quantify numerically the plate area wetted by the drop as well as the drop gas-liquid interface area exposed to the fluid flow. We furthermore assess the importance of flow deformation in modulating the drop shape. Using the combined experimental-numerical approach, we make a first assessment of the suitability of using pure air/water properties for simulations of self-cleaning in two-phase heat exchangers.

2 Methods

2.1 Experimental

The experimental procedure is designed to establish the equilibrium contact angles of water, with and without a solute containing an aromatic ring, on two steel plates of different surface modification. The experiment is performed for plate inclinations from 0 to 20°.

The plates are the same as those investigated by Maggiolo et al. (2019a). The silicon-based treatments of the plates are performed using a liquid precursor applied using a wet chemical process, followed by a thermal curing step. The resulting ceramic coatings are purely inorganic silicon oxides with an average thickness of 400 nm, where one of the plates is more hydrophilic and the other is more hydrophobic.

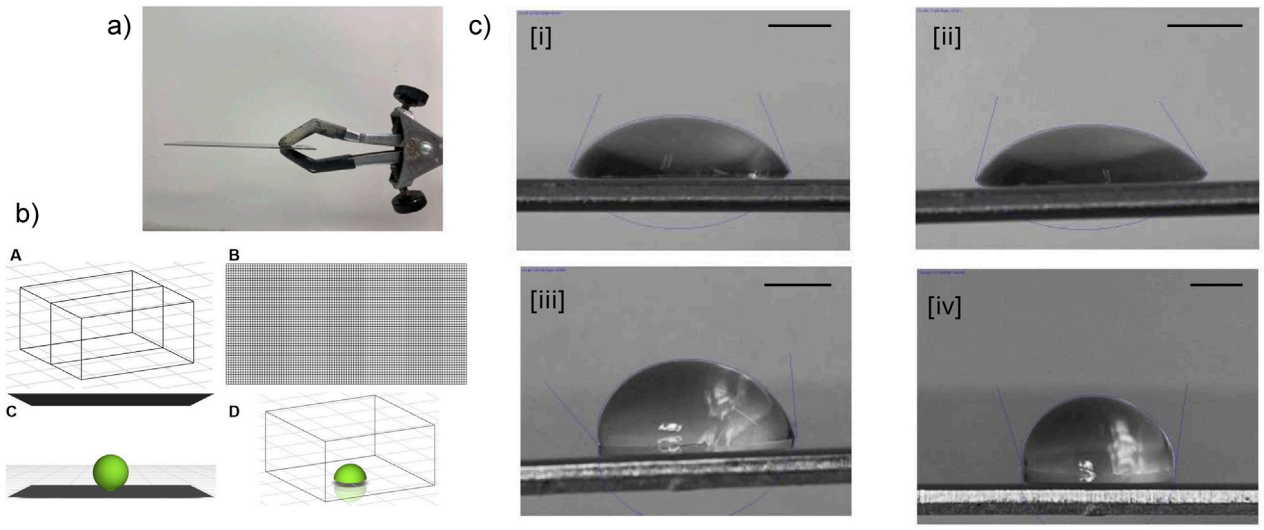

FIGURE 1
(a) Photo of experimental setup; **(b)** Illustrations of computational setup – (A) the doubly periodic box domain with plates at the bottom and top, (B) the mesh resolution in the plane drawn in the middle of panel (A,C) drop placed on the bottom wall as the initial condition, (D) snapshot from a simulation with flow; **(c)** Sample photos from the experimental tests, along with their extracted apparent advancing and receding contact angles: [i] hydrophilic coating, 0-degree inclination, pure distilled water; θ_a = 67.98, θ_r = 67.68, [ii] hydrophilic coating, 8-degree inclination, distilled water with benzoic acid; θ_a = 73.55, θ_r = 57.92, [iii] hydrophobic coating, 16-degree inclination, pure distilled water; θ_a = 127.77, θ_r = 87.18, [iv] hydrophobic coating, 6-degree inclination, distilled water with benzoic acid; θ_a = 106.73, θ_r = 97.67. The horizontal scale bars in panels [i-iv] illustrate a length corresponding to 1 mm.

Two solutions are employed in the experiments: pure distilled water and distilled water with dissolved benzoic acid. We employ a concentration of 200 mg/L (prepared by dissolving 50 mg benzoic acid in 250 mL distilled water). The solubility of benzoic acid in water is 3,400 mg/L at 302 K (PubChem, 2019).

The metal plate is fixed on a clamp with the desired inclination/tilting angle, as illustrated in Figure 1a. Drops are placed on the surface by a pipette. The droplet contact angles are analyzed for every 2° inclination of the metallic plate. At 20°, the droplet starts to slide on the hydrophilic coating. Three repeated trials are conducted for every inclination of the metallic plates to quantify the repeatability. The volume of a single drop is calculated by counting the number of drops it takes to fill a volume of 10 mL. This test was also repeated thrice. 210 drops were required to fill a volume of 10 mL, hence the volume of a single drop is approximately 0.05 mL.

Images of the droplets are taken during the experiment and thereafter converted into grayscale images using Matlab R2020b. The grayscale images are analyzed using ImageJ with the DropSnake plug-in to determine the contact angles from a piecewise polynomial fit (ImageJ software, 2015). More precisely, the DropSnake method is based on B-spline snakes (active contours) to shape the drop (DropSnake software, 2016).

It should be stressed here that we will be referring to the different contact angles on the downhill and uphill sides of the drop when the plate is tilted as advancing and receding contact angles, respectively. As these terms are most often associated with a moving drop (and a moving contact line), a more correct term would perhaps be apparent or static advancing and receding contact angles (Lam et al., 2002; Lam et al., 2001; Tadmor, 2004). However, we shall use the shorter nomenclature to facilitate the presentation, whilst reminding the reader that the contact line remains pinned for all scenarios investigated in the current work.

2.2 Simulations

Computational fluid dynamics (CFD) simulations are performed using the Volume-of-Fluid (VOF) method (Renardy et al., 2001), which is a one-fluid multiphase Direct Numerical Simulation (DNS) methodology based on the Navier-Stokes equations (continuity (Equation 1) and momentum balance (Equation 2)):

$$\nabla \cdot \boldsymbol{v} = 0 \tag{1}$$

$$\rho\left(\frac{\partial \boldsymbol{v}}{\partial t} + \boldsymbol{v} \cdot \frac{\partial \boldsymbol{v}}{\partial \boldsymbol{x}}\right) = -\nabla p + \nabla \cdot \left(\mu\left[\nabla \boldsymbol{v} + (\nabla \boldsymbol{v})^{\mathrm{T}}\right]\right) + \rho \boldsymbol{g} + \frac{\sigma\rho(\nabla \cdot \alpha)\nabla\alpha}{\frac{1}{2}\left(\rho_g + \rho_l\right)} \tag{2}$$

Here, $\boldsymbol{v}$ is the velocity (m/s), p is the pressure (Pa), $\boldsymbol{g}$ is the gravitational acceleration vector (m/s^2), σ is the surface tension at the gas-liquid interface (N/m), α is the volume fraction of liquid (–), and the one-fluid properties (density, ρ, and viscosity, μ) are obtained using Equations 3, 4:

$$\rho = \alpha\rho_l + (1-\alpha)\rho_g \tag{3}$$

$$\mu = \alpha\mu_l + (1-\alpha)\mu_g \tag{4}$$

The volume fraction field is described by the following advection equation:

$$\frac{\partial \alpha}{\partial t} + \nabla \cdot (\alpha \boldsymbol{v}) = 0 \tag{5}$$

The computational domain is a box of $10 \times 5 \times 10$ mm^3, with periodic boundary conditions in the x and z directions, and no-slip wall boundary conditions on the top and bottom in the y direction. The plate-to-plate distance is 5 mm. A pressure gradient of 0.143 Pa/m, chosen to attain an approximate velocity of 0.02 m/s (as in Maggiolo et al. (2019a)), is applied to drive the flow in the z direction.

In the cell layer next to the wall boundaries, the contact angle prescribed from experiments is used to set the local curvature of the interface such that the experimentally determined wall adhesion is recreated in the simulation. In our previous work, we employed a density-dependent function to recreate the macroscopically observed equilibrium contact angle in a Lattice-Boltzmann framework (Maggiolo et al., 2019a; Maggiolo et al., 2019b). The herein adopted approach enables us to prescribe the experimentally observed contact angle directly (rather than indirectly via parameter tuning) and to use the physically correct density and viscosity ratios without stability problems (Aidun and Clausen, 2010).

The initial condition is that a spherical drop of 2 mm diameter is placed on top of the bottom wall in a quiescent fluid. This drop size is chosen as it is associated with the onset of the self-cleaning mechanism on the hydrophobically treated plates (Maggiolo et al., 2019a). Thereafter, the solution is advanced in time while monitoring the magnitude of the total gas-liquid interface. The area of the interface is obtained from the solver fields by creating an iso-surface at $\alpha = 0.5$ through interpolation of node values. At the same time, the area of the plate wetted by a drop is obtained as $\sum_i \alpha_i A_i$, where the sum is over all wall faces i on the bottom plate in the computational domain, and A_i is the local face area. The material properties used in the simulations are: $\rho_g = 1.225$ kg/m^3, $\rho_l = 998.2$ kg/m^3, $\mu_g = 1.7894.10^{-5}$ Pa,s, $\mu_l = 0.001003$ Pa,s, and $\sigma = 0.072$ N/m. Note that, as benzoic acid is a weak surfactant and water at neutral pH is used in conjunction with low concentration, the surface tension value of the system is kept constant. The role of benzoic acid addition is thus to alter the effective contact angle at the three-phase contact line, as prescribed by the measurement data. When the areas have stabilized after an initial transient, their values are recorded.

The solver used is the pressure-based Navier-Stokes solver of ANSYS Fluent 2022. R1, which employes the SIMPLE scheme for the pressure-velocity coupling, the PRESTO! scheme for pressure discretization, the second-order upwind scheme for the convective term in Equation 2 and the second-order central differencing scheme for the diffusion term. First-order implicit time stepping is used with a fixed time step that always maintains a Courant number less than 0.25. For Equation 5, the Geo-Reconstruct scheme is used for the spatial discretization and an explicit scheme for the temporal discretization.

The computational mesh contains 500,000 hexahedral cells at a resolution of $\Delta x = 0.1$ mm. The domain, the mesh, the initial solution, and a sample snapshot of an instantaneous solution are visualized in Figure 1b.

3 Results and discussion

3.1 Experimental results

Examples of experimental photos with identified apparent advancing and receding contact angles are provided in Figure 1c, for both plates and at varying inclination. The main trends can be discerned from the chosen examples: drops on a hydrophilically treated plate exhibit lower contact angles than the same drop on a hydrophobically treated plate; plate inclination induces a difference between advancing and receding contact angles on both plates (increasing the former and decreasing the latter); and addition of benzoic acid to the distilled water tends to decrease contact angles. The contact angle was not measured on uncoated steel plates but is expected to be in the interval 68°–113° (Maggiolo et al., 2019a).

The complete experimental data set is presented in Figures 2a, b for the plate with hydrophilic coating, and in Figures 2c, d for the plate with hydrophobic coating. The error bars indicate the standard deviation from three repeated experiments. It is seen that, at 20° inclination, the drop has a tendency to start to slide on the plate, and this phenomenon is reflected in a sharp increase in the uncertainty estimate.

Overall, the decrease due to the presence of benzoic acid in advancing and receding contact angles appears to be relatively constant when varying the inclination of the hydrophilic plate. It is approximately 4.0° for the advancing and 3.4° for the receding contact angles, respectively. On the hydrophobic plate, the differences are initially larger: for inclinations up to approximately 5°, the difference is 12.3° in contact angle on both sides (advancing and receding). For larger inclinations, between 5 and 10°, the difference decreases and starts to deviate on the advancing and receding sides: 11.2° for the advancing contact angle and 10.4° for the receding contact angle. The difference invoked by the addition of benzoic acid remains relatively constant for inclinations up to 20°, whereas it more or less vanishes for the receding contact angle at the higher inclinations.

The hydrophilicity of the silicon-based coating is governed by surface silanol (Si-OH) groups that hydrogen-bond with water, whereas hydrophobic behavior can arise from reduced -OH density or surface chemistry that diminishes water adsorption (Kolman and Abbas, 2019). Upon addition of benzoic acid, the wettability may change either due to surface chemistry effects (i.e., effects at the liquid-solid interface) or surfactant effects (i.e., effects at the gas-liquid interface). If the benzoic acid molecules adsorb on the silica coating, its addition tends to increase the contact angle (Satyarthy et al., 2025; Kolman and Abbas, 2019; Terra et al., 2022; Staniscia et al., 2022). If, on the other hand, the benzoic acid preferentially accumulates at the gas-liquid interface (since the aromatic ring is hydrophobic), modification of the air-liquid surface tension becomes more dominant and the contact angle tends to decrease (Satyarthy et al., 2025; Kolman and Abbas, 2019; Staniscia et al., 2022; Ghzaoui, 1999). The present results, with a decrease in contact angle at the introduction of benzoic acid to the distilled water, imply that the coatings applied offer little chemical affinity for benzoic acid and that the mild surfactant effects are instead dominant (Staniscia et al., 2022).

The contact angle hysteresis (defined as the difference between the advancing and the receding static contact angles) is shown in Figure 2e. The hysteresis increases with increasing the tilting angle of the plate, as is expected for a pinned droplet able to balance its own weight by distorting (Quéré et al., 1998). For the plate with the hydrophilic coating, the addition of benzoic acid has no significant effect. This observation indicates that benzoic acid does not interact

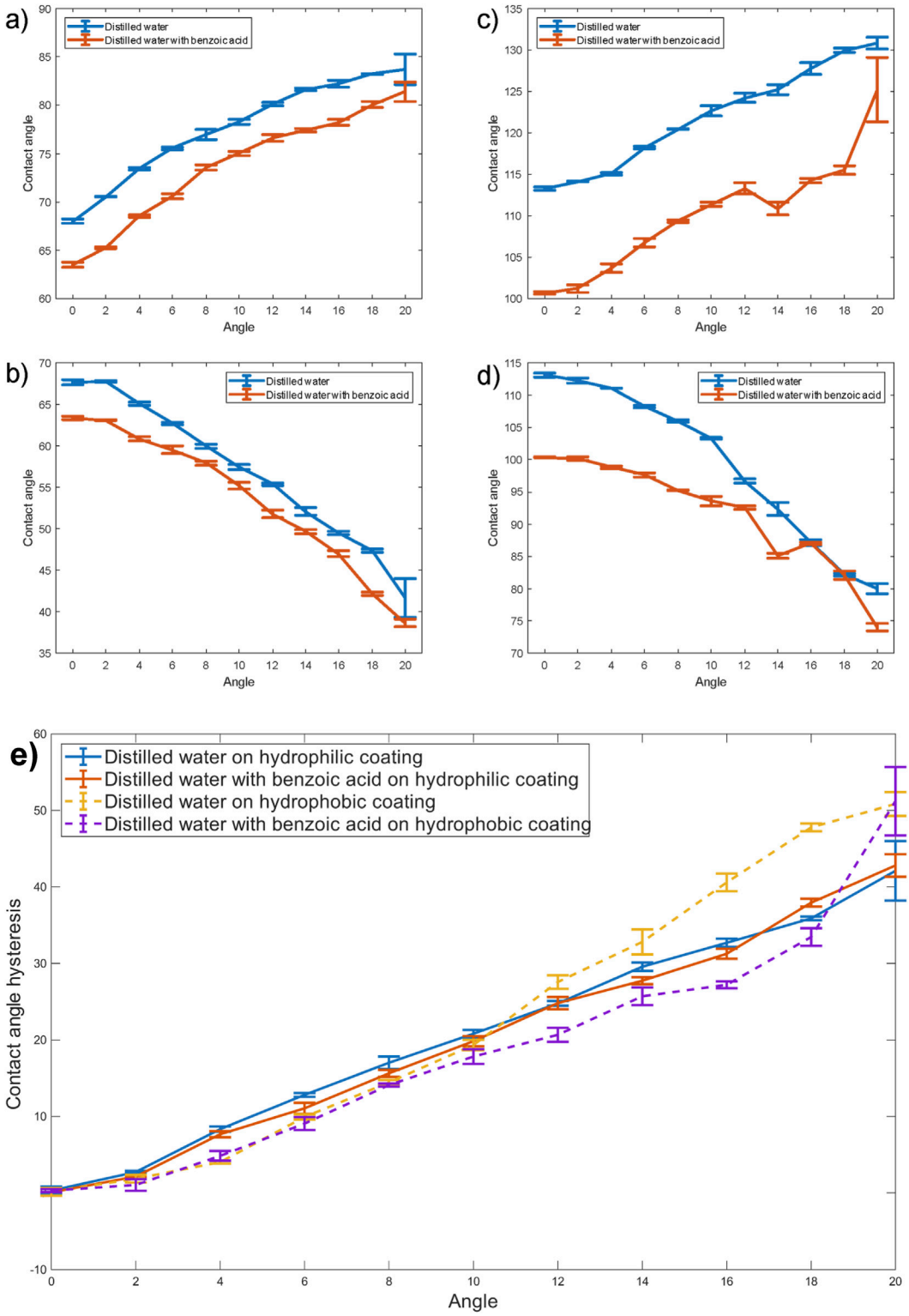

FIGURE 2
Apparent (static) contact angles at inclination angles from 0 to 20°: **(a)** advancing and **(b)** receding contact angles on the plate with hydrophilic coating, **(c)** advancing and **(d)** receding contact angles on the plate with hydrophobic coating, and **(e)** contact angle hysteresis.

strongly with the solid surface, and hence the contact line pinning is due to microscopic surface roughness or chemical heterogeneity (e.g., patches of silanol groups) unaffected by the benzoic acid in the liquid (Li et al., 2014). The contact angle hysteresis is similarly unaffected by the addition of benzoic acid on the hydrophobic plate at low-to-moderate tilting angles. It is noted that the hysteresis is lower on the hydrophobic coating than on the hydrophilic one in this range, which supports the conclusion from Maggiolo et al.

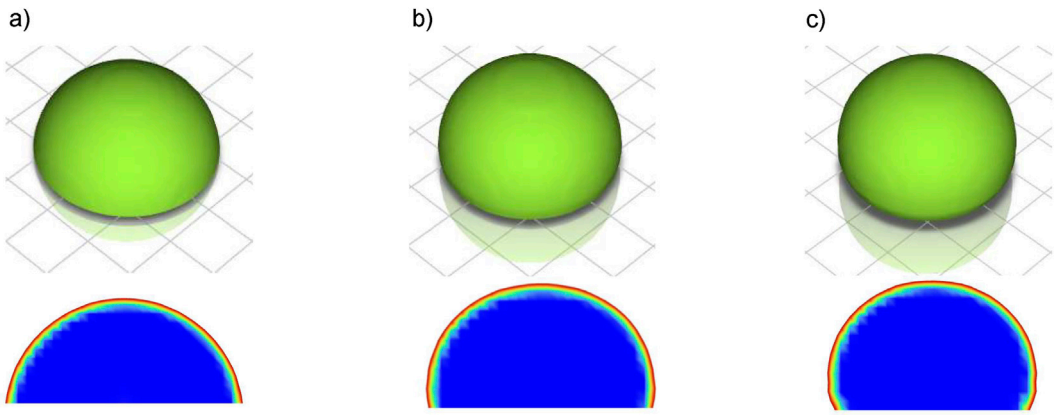

FIGURE 3
Stable droplet shapes in pressure-driven flow as predicted for contact angles of **(a)** 85° [reference case], **(b)** 100° [water with benzoic acid on hydrophobically modified plate], and **(c)** 113° [pure water on hydrophobically modified plate]. Top row illustrates the gas-liquid interface (α = 0.5 iso-surfaces). Bottom row illustrates the drop shape in the *yz* plane (colored by α, with blue = 1 and red = 0).

(2019a) that drops are more mobile on the hydrophobic plates. At larger tilting angles, the hysteresis is reduced upon addition of benzoic acid on the hydrophobic plate, indicating either adsorption of benzoic acid molecules onto the SiO_2-surface (the carboxyl group could attach to polar -OH groups, exposing the hydrophobic benzene ring and thereby increasing the effective hydrophobicity of the surface) or modest benzoic acid accumulation at the liquid-air interface (Kamieński et al., 1965; Park et al., 2022).

In conclusion, we find that on the hydrophilically modified plate, the drops with pure distilled water and drops with benzoic acid behave identically, apart from a constant offset in the equilibrium advancing and receding contact angles on the order of 3–5°. On the hydrophobically modified plate, the addition of benzoic acid has a more pronounced effect, decreasing the equilibrium advancing and receding contact angles by approximately 11–12° at low plate inclination. As the plate inclination is increased, the effect of the benzoic acid on the receding contact angle more or less disappears, whereas the influence on the advancing one remains relatively constant. Contact angle hysteresis is relatively unaffected by benzoic acid addition on both plates, except at high tilting angles on the hydrophobic plate where hysteresis is reduced.

3.2 Simulation results

The purpose of the numerical simulations is to assess the role of the fluid flow in shaping the moving drops with a prescribed equilibrium contact angle in the system. The lateral and streamwise periodicity implies that the drop is moving in a system where the distance between adjacent drops is approximately 5 drop diameters, which agrees with the experimental observations of Maggiolo et al. (Maggiolo et al., 2019a) for industrial two-phase plate heat exchangers. Instantaneous visualizations of iso-surfaces representing the gas-liquid interface at quasi-steady conditions are provided in Figure 3 for prescribed contact angles at the wall of 85, 100, and 113°. The 85-degree case reflects one of the cases investigated in Maggiolo et al. (2019a) and is included here as a reference case, whereas the 113-degree case represents pure distilled water and the 100-degree case water with benzoic acid. As the contact angle increases, the drop becomes more spherical. This observation is in good agreement with the analysis in Maggiolo et al. (2019a), which showed that increased hydrophobicity promoted the formation of small, spherical-like, motile droplets under similar flow conditions.

The simulations enable quantification of the droplet surface area and how it changes with changing the drop-plate interaction in the fully resolved, three-dimensional transient flow field. Figure 4a depicts the increase in the plate area wetted by the drop, as compared to a spherical-cap drop of the same radius as the initial drop. The more efficient the wetting of the plate (i.e., the lower the equilibrium contact angle), the larger the wetted area. These quantitative results align well with the qualitative observations from Figure 3. At the same time, Figure 4b displays the decrease of the surface area of the drop exposed to the flow, as compared to the nominal surface area of the initial, completely spherical drop. The deformation of the drop due to the interaction with the plate and the flow leads to a decrease in the gas-liquid interface exposed to the flow, whereas this effect is relatively mild for the investigated parameter range. Finally, in Figure 4c, the variation of the total drop surface area (sum of wall-wetted area and gas-liquid interface exposed to the flow) with the equilibrium contact angle is shown. In all cases, the deformation of the drop from the perfect spherical shape implies an effective increase in the total drop surface area, and this effect is more pronounced for the least hydrophobic plate. These results underline the role of the hydrophobicity of the plate in promoting the formation of close-to-spherical drops moving over the plate surface.

We further extract the increase in exposed gas-liquid interfacial area due to the flow, as obtained from comparisons of simulations with an applied pressure gradient in the streamwise direction to results obtained without any prescribed macroscopic motion (i.e., zero pressure gradient in the streamwise periodic direction). It is found that this increase is 0.065% at 85° contact angle, 0.28% at 100°, and 0.42% at 113°. Evidently, the role of the flow in modulating

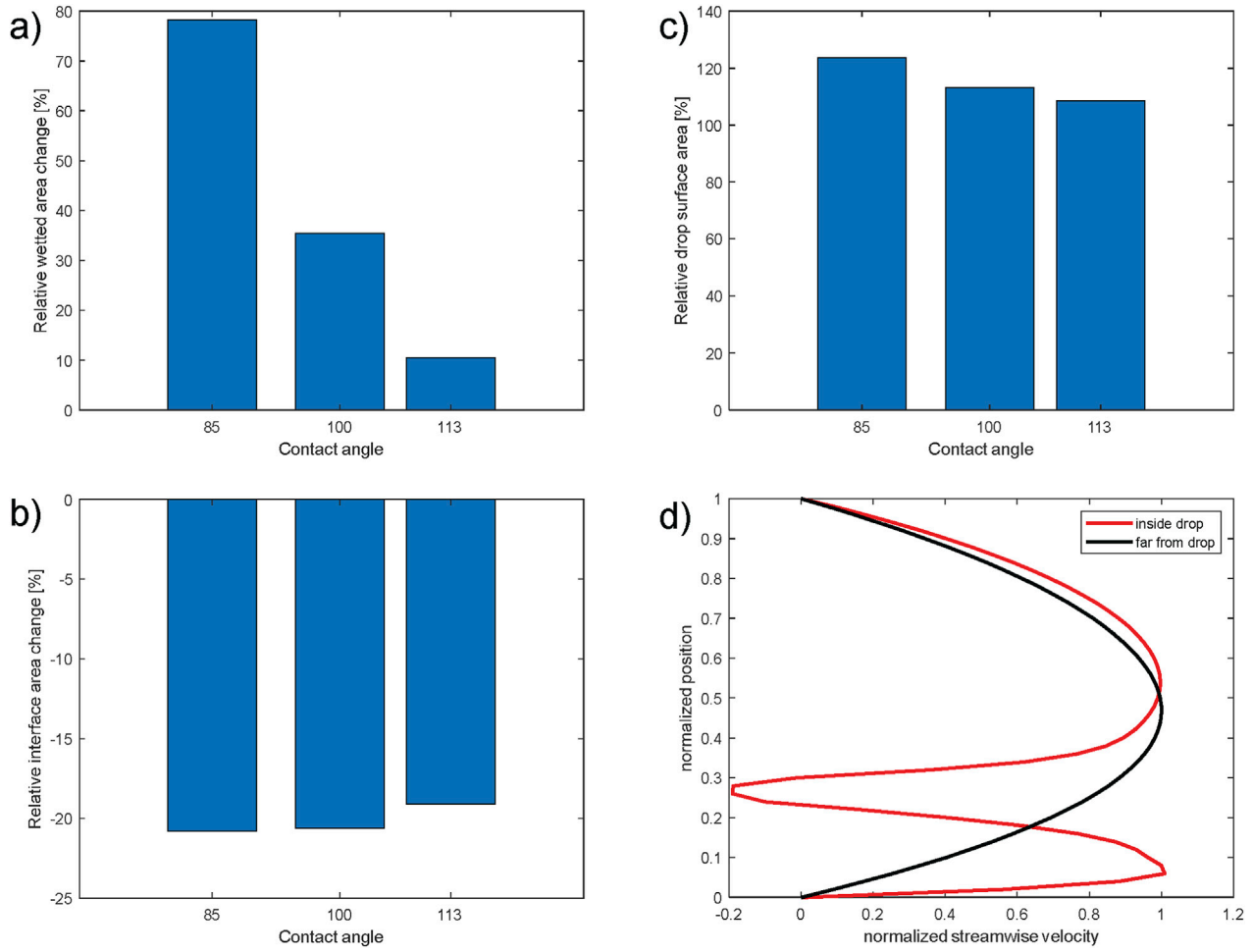

FIGURE 4
(a) Relative change [%] of the wetted area on the plate, as compared to a spherical-cap drop of the same radius as the initial drop, as a function of the contact angle prescribed at the plate surface. **(b)** Relative change [%] of the gas-liquid interface area from the surface area of a spherical drop of the same volume, as a function of the contact angle prescribed at the plate surface. **(c)** Total surface area [%] (sum of gas-liquid interface area and wall-wetted area) normalized by the surface area of a spherical drop of the same volume, as a function of the contact angle prescribed at the plate surface. **(d)** Normalized streamwise velocity ($v_z/v_{z,max}$) as a function of normalized position (y/h) for the case where the contact angle is 113° [pure water on hydrophobically modified plate]. The red line is drawn through the center of the drop and the black line is drawn far away from the drop (in the middle of the xy plane at the periodic boundary in the z direction).

the gas-liquid interface is not strong at the current conditions. To substantiate this analysis, we also analyze the streamwise velocity profile along a line from plate to plate, through the middle of the drop, and contrast the profile there to that along a line far away from the drop. The outcome of this analysis is shown in Figure 4d. The streamwise velocity far away from the drop exhibits a characteristic parabolic shape. The velocity profile along the line cutting through the drop has a parabolic-like shape above the drop, with the added complexity arising from the internal circulation within the moving drop that gives rise to negative flow in the streamwise direction just inside the gas-liquid interface at the top of the drop. The role of the flow outside the drop is thus to impart motion in the streamwise direction, similar to that of the gas phase, along with inducing internal circulation. The distorting inertial forces are not significant compared to the restoring surface tension forces at the present conditions, and so the deformation of the droplet shape due to the flow is minimal, as expected.

In conclusion, we find that the drop is more spherical at higher plate hydrophobicity, such that the hydrophobically treated plate promotes the formation of almost-spherical droplets. The disturbances induced by the flow on the droplet shape are not significant at the current operating conditions. The role of benzoic acid addition to a pure distilled water drop is to cause a more pronounced spreading of the drop on the plate, however the differences are not large (cf. panels (b) and (c) in Figure 3). The more pronounced wetting of the plate is associated with a decrease in the gas-liquid interface area exposed to the flow. Therefore, the role of a component such as benzoic acid is to decrease the effectiveness of the two-phase heat exchanger in promoting the flow structure needed to maintain self-cleaning functionality. However, it is also clear from the current results that the effect of benzoic acid is relatively minor: as long as the equilibrium contact angles are within the hydrophobic range, the overall characteristics of the drop properties and behaviors are seemingly maintained.

4 Conclusion

Self-cleaning effects can be induced in two-phase droplet-laden flows if the system characteristics and operating conditions promote the emergence of small, spherical, motile drops. The underlying principles have been shown in experiments using complex chemical makeup and reproduced in numerical simulations using physicochemical properties representative of air-water systems. In the present work, we experimentally and numerically investigate the addition of benzoic acid to an otherwise pure air-water system on the equilibrium contact angles of drops placed on hydrophilically and hydrophobically modified plates, at varying plate inclinations.

We show that the addition of benzoic acid produces a constant offset in the equilibrium advancing and receding contact angles on the order of 3–5° on the hydrophilically modified plate. On the hydrophobically modified plate, the addition of benzoic acid has a more pronounced effect, in that it decreases the equilibrium advancing and receding contact angles by approximately 11–12° at low plate inclination. The effect on the advancing contact angle remains at all tested inclinations, whereas the effect on the receding one disappears as the inclination is increased.

The simulations show that the hydrophobically treated plate, as expected, produces more spherical drops that are relatively immune to flow-induced disturbances. The addition of benzoic acid reverts the system somewhat to the behavior of a less hydrophobic one, by increasing the wetting of the drop on the surface and decreasing the flow-exposed gas-liquid interface. The effect is however not strong, and it is concluded that two-phase heat exchangers relying on self-cleaning mechanisms can still be expected to be relatively immune to the dissolution of amphiphilic impurities containing a benzene ring, at least provided that it comes with a carboxyl substituent.

Data availability statement

The raw data supporting the conclusions of this article will be made available by the authors, without undue reservation.

Author contributions

SK: Conceptualization, Data curation, Formal Analysis, Investigation, Methodology, Software, Validation, Visualization, Writing – original draft. HS: Conceptualization, Formal Analysis, Funding acquisition, Investigation, Methodology, Project administration, Resources, Software, Supervision, Visualization, Writing – review and editing.

Funding

The author(s) declared that financial support was received for this work and/or its publication. Financing of this work by The Centre for Combustion Science and Technology (CECOST) is gratefully acknowledged.

Conflict of interest

The author(s) declared that this work was conducted in the absence of any commercial or financial relationships that could be construed as a potential conflict of interest.

Generative AI statement

The author(s) declared that generative AI was not used in the creation of this manuscript.

Any alternative text (alt text) provided alongside figures in this article has been generated by Frontiers with the support of artificial intelligence and reasonable efforts have been made to ensure accuracy, including review by the authors wherever possible. If you identify any issues, please contact us.

Publisher's note

References

Aidun, C. K., and Clausen, J. R. (2010). Lattice-boltzmann method for complex flows. *Annu. Rev. Fluid Mech.* 42, 439–472. doi:10.1146/annurev-fluid-121108-145519

Al-Sharafi, A., Yilbas, B. S., Sahin, A. Z., and Ali, H. (2017). Flow field inside a sessile droplet on a hydrophobic surface in relation to self cleaning applications of dust particles. *J. Heat Transf.* 139, 042003. doi:10.1115/1.4035281

Alamry, K. A., Khan, A., Aslam, J., Hussein, M. A., and Aslam, R. (2023). Corrosion inhibition of mild steel in hydrochloric acid solution by the expired Ampicillin drug. *Sci. Rep.* 13, 6724. doi:10.1038/s41598-023-33519-y

Cohr, K. H., and Stokholm, J. (1979). Toluene: a toxicologic review. *Scand. J. Work, Environ. and Health* 5, 71–90. doi:10.5271/sjweh.2664

DropSnake software (2016). Available online at: http://bigwww.epfl.ch/demo/dropanalysis/soft.

Ghzaoui, El (1999). Relation between the variation of the contact angle and the adhesion force between silica surfaces. *J. Colloid Interface Sci.* 216, 432–435. doi:10.1006/jcis.1999.6324

Hassan, G., Yilbas, B. S., Bahatab, S., Al-Sharafi, A., and Al-Qahtani, H. (2020). A water droplet-cleaning of a dusty hydrophobic surface: influence of dust layer thickness on droplet dynamics. *Sci. Rep.* 10, 14746. doi:10.1038/s41598-020-71743-y

ImageJ software (2015). Available online at: https://imagej.nih.gov/ij/.

Jordan, C. A., and Akay, G. (2013). Effect of CaO on tar production and dew point depression during gasification of fuel cane bagasse in a novel downdraft gasifier. *Fuel Process. Technol.* 106, 654–660. doi:10.1016/j.fuproc.2012.09.061

Kamieński, B., and Krauss, E. (1965). Surface potential and surface tension of aqueous solutions of phenylarsonic acid and derivatives. *Electrochimica Acta* 10, 879–881. doi:10.1016/0013-4686(65)80052-4

Kim, S., Marcano, M. C., and Becker, U. (2021). Effects of hydroxyl and carboxyl functional groups on calcite surface wettability using atomic force microscopy and density functional theory. *ACS Earth Space Chem.* 5, 2545–2554. doi:10.1021/acsearthspacechem.1c00240

Kochkodan, V., Johnson, D. J., and Hilal, N. (2014). Polymeric membranes: surface modification for minimizing (bio)colloidal fouling. *Adv. Colloid Interface Sci.* 206, 116–140. doi:10.1016/j.cis.2013.05.005

Kolman, K., and Abbas, Z. (2019). Molecular dynamics exploration for the adsorption of benzoic acid derivatives on charged silica surfaces. *Colloids Surfaces A* 578, 123635. doi:10.1016/j.colsurfa.2019.123635

Lam, C. N. C., Ko, R., Yu, L., Ng, A., Li, D., Hair, M., et al. (2001). Dynamic cycling contact angle measurements: study of advancing and receding contact angles. *J. Colloid Interface Sci.* 243, 208–218. doi:10.1006/jcis.2001.7840

Lam, C. N. C., Wu, R., Li, D., Hair, M. L., and Neumann, A. W. (2002). Study of the advancing and receding contact angles: liquid sorption as a cause of contact angle hysteresis. *Adv. Colloid Interface Sci.* 96, 169–191. doi:10.1016/s0001-8686(01)00080-x

Li, Y. F., Sheng, Y. J., and Tsao, H. K. (2014). Solute concentration-dependent contact angle hysteresis and evaporation stains. *Langmuir* 30, 7716–7723. doi:10.1021/la501438k

Li, M-J., Tang, S-Z., Wang, F-L., Zhao, Q-X., Tao, W-Q., et al. (2017). Gas-side fouling, erosion and corrosion of heat exchangers for middle/low temperature waste heat utilization: a review on simulation and experiment. *Appl. Therm. Eng.* 126, 737–761.

Liang, B., and Clarens, A. F. (2018). Interactions between stratigraphy and interfacial properties on flow and trapping in geological carbon storage. *Water Resour. Res.* 54, 72–87. doi:10.1002/2017wr021643

Loomis, D., Guyton, K. Z., Grosse, Y., El Ghissassi, F., Bouvard, V., Benbrahim-Tallaa, L., et al. (2017). Carcinogenicity of benzene. *Lancet* 18, 1574–1575. doi:10.1016/S1470-2045(17)30832-X

Lu, S., Cheng, Y., Dong, J., and Li, X. (2024). Molecular origin for pH-responsive wormlike micelles of zwitterionic surfactants triggered by aromatic acid derivatives. *ChemPhysMater* 3, 230–238. doi:10.1016/j.chphma.2024.02.002

Maggiolo, D., Seemann, M., Thunman, H., Santos, O., Larsson, A., Sasic, S., et al. (2019a). Self-Cleaning surfaces for heat recovery during industrial hydrocarbon-rich gas cooling: an experimental and Numerical Study. *AIChE J.* 65, 317–325. doi:10.1002/aic.16394

Maggiolo, D., Sasic, S., and Ström, H. (2019b). Self-cleaning compact heat exchangers: the role of two-phase flow patterns in design and optimization. *Int. J. Multiph. Flow* 112, 1–12. doi:10.1016/j.ijmultiphaseflow.2018.12.006

Melo, L., Bott, T. R, and Bernardo, C. A (1988). *Fouling science and technology*. Kluwer Academic Publishers.

Müller-Steinhagen, H., Malayeri, M. R., and Watkinson, A. P. (2011). Heat exchanger fouling: mitigation and cleaning strategies. *Heat. Transf. Eng.* 32, 189–196. doi:10.1080/01457632.2010.503108

Park, S. C., Kim, Y. H., Jang, J. G., Cho, H. R., Kwak, H. J., Kim, J. H., et al. (2022). Dynamic contact angles and pressure drop at moving contact lines of water/ethanol mixture slug in hydrophobic capillary tubes *via* synchrotron x-ray imaging. *Phys. Fluids* 34, 032117. doi:10.1063/5.0076779

Phan, C. M. (2018). "Ionization of surfactants at the air–water interface," in *Physical chemistry of gas-liquid interfaces, developments in physical and theoretical chemistry*, 79–104.

PubChem (2019). *Benzoic Acid Compound Summary*. Bethesda, MD: National Library of Medicine. Available online at: https://pubchem.ncbi.nlm.nih.gov/compound/Benzoic-Acid.

Quéré, D., Azzopardi, M. J., and Delattre, L. (1998). Drops at rest on a tilted plane. *Langmuir* 14, 2213–2216. doi:10.1021/la970645l

Renardy, M., Renardy, Y., and Li, J. (2001). Numerical simulation of moving contact line problems using a volume-of-fluid method. *J. Comput. Phys.* 171, 243–263. doi:10.1006/jcph.2001.6785

Santos, O., Nylander, T., Rosmaninho, R., Rizzo, G., Yiantsios, S., Andritsos, N., et al. (2004). Modified stainless steel surfaces targeted to reduce fouling – surface characterization. *J. Food Eng.* 64, 63–79. doi:10.1016/j.jfoodeng.2003.09.013

Satyarthy, S., Cheng, M., and Ghosh, A. (2025). Investigating benzoic acid derivatives as potential atomic layer deposition inhibitors using nanoscale infrared spectroscopy. *Nanomaterials* 15, 164. doi:10.3390/nano15030164

Staniscia, F., Guzman, H. V., and Kanduč, M. (2022). Tuning contact angles of aqueous droplets on hydrophilic and hydrophobic surfaces by surfactants. *J. Phys. Chem. B* 126, 3374–3384. doi:10.1021/acs.jpcb.2c01599

Tadmor, R. (2004). Line energy and the relation between advancing, receding, and young contact angles. *Langmuir* 20, 7659–7664. doi:10.1021/la049410h

Terra, N., Ligiero, L. M., Molinier, V., Giusti, P., Agenet, N., Loriau, M., et al. (2022). Characterization of crude oil molecules adsorbed onto carbonate rock surface using LDI FT-ICR MS. *Energy and Fuels* 36, 6159–6166. doi:10.1021/acs.energyfuels.2c00840

Thunman, H., Seemann, M., Berdugo Vilches, T., Maric, J., Pallares, D., Ström, H., et al. (2018). Advanced biofuel production *via* gasification – lessons learned from 200 man-years of research activity with Chalmers' research gasifier and the GoBiGas demonstration plant. *Energy Sci. and Eng.* 6, 6–34. doi:10.1002/ese3.188

Zhang, M., Feng, S., Wang, L., and Zheng, Y. (2016). Lotus effect in wetting and self-cleaning. *Biotribology* 5, 31–43.

Zhang, K., Li, Z., Maxey, M., Chen, S., and Karniadakis, G. E. (2019). Self-Cleaning of hydrophobic rough surfaces by coalescence-induced wetting transition. *Langmuir* 35, 2431–2442. doi:10.1021/acs.langmuir.8b03664